# Broken Symmetry in the Density of Electronic States of an Array of Quantum Dots As Computed for Scanning Tunneling Microscopy†

**F. Remacle‡**

*Département de Chimie, B6, Université de Liège, B 4000 Liège, Belgium*

**R. D. Levine***

*The Fritz Haber Research Center for Molecular Dynamics, The Hebrew University, Jerusalem 91904, Israel, and Department of Chemistry and Biochemistry, University of California Los Angeles, Los Angeles, California 90095*

*Received: April 3, 2000; In Final Form: July 11, 2000*

Broken symmetry is characteristic of arrays of quantum dots and can be observed in the failure of selection rules of optical spectroscopy or in the dielectric properties. Here we discuss scanning tunneling spectroscopy, where electrons are detached or attached. In the lowest order of description (sometimes known as Koopmans theorem), the orbitals of a system are regarded as given and one adds or removes electrons from these orbitals. If one has a half-full band of states whose energies have a reflection symmetry about the center, the density of states should be symmetric about the energy of the highest occupied state. Features that are special to arrays of nanodots and lead to the breaking of the expected symmetry are identified. Computations of the density of states of an array of Ag nanodots that are in accord with the available experimental observations are also provided. For a disordered array, the response of the STM probe can be qualitatively different at different lattice points and we interpret this in terms of a change in the nature of the ground electronic state of the array when it is more disordered.

## 1. Introduction

In scanning tunneling[7,16] (STM) experiments[2,3,8,15,18] one removes or adds electrons to the sample, depending on the direction of the applied voltage. In this sense, scanning tunneling spectroscopy is analogous to photoelectron spectroscopy, (where an electron is removed) or to attachment experiments (where it is added). In a simple one electron orbital picture, electrons are removed from or added to given orbitals of the system. The orbitals of the $n-1$, $n$, and $n+1$ electron systems are, in this simple picture, the same. In particular, the lowest ionization voltage is the energy of the highest occupied molecular orbital (HOMO) while an added electron is placed in the lowest unoccupied molecular orbital (LUMO). This picture is retained even when the orbitals are computed such that an electron moves in the mean field of the other electrons and the quantitative statement is often known as Koopmans theorem.[22] It is recognized to be an approximation, but it is a very useful approximation because it allows us to think in simple terms about adding or removing an electron. In this paper we argue that this approximation will break down for arrays of quantum dots. We discuss what is special about quantum dots that makes the breakdown serious and present computational results in support of our physical considerations. We also suggest that there is experimental evidence[15,18] that can be explained by our considerations.

The implications of Koopmans theorem are particularly easy to visualize for such systems (e.g., molecules with alternant symmetry[22,23]) where the energies of the occupied and unoccupied molecular orbitals have a mirror symmetry about their midpoint. For every energy of removing an electron there is the mirror image energy for adding an electron. The "density of states" as measured by scanning tunneling spectroscopy will therefore show mirror symmetry when plotted as a function of the voltage difference between the sample and the tip. It is the breakdown of this expected symmetry that is the subject of the present analysis.

We specifically identify one particular characteristic of quantum dots as primarily responsible for the breakdown in symmetry. This is their so-called "charging energy", which is atypically low (0.338 eV for the Ag nanodots[15,18] that we will specifically try to simulate. It is low when it is compared to the corresponding values for most atoms). The charging energy is itself measured by scanning tunneling spectroscopy when the lattice is so very expanded that the dots are not interacting. It is the energy required to add another electron to an isolated single dot. It takes energy because this extra electron is repelled by the electrons already in the dot. The dimensions of a dot are large compared to an atom and this means that the charging energy is not high. But it is finite and measurable. In metals, the finite charging energy is known as the "Coulomb blockade" to conduction.[14,19,31]

The low charging energy also means that electrons on adjacent dots are not strongly repelling. We include this repulsion in the Hamiltonian that is used.

Another experimental observation[15] that we would like to explain is the scanning tunneling spectroscopy of expanded lattices. Often, up to the inevitable noise, the spectrum is the same for different positions of the lattice. It is, however, found that when there is more variability in the size of the individual

† Part of the special issue "C. Bradley Moore Festschrift".

* Corresponding author. Fax: 972-2-6513742. E-mail: rafi@fh.huji.ac.il.
‡ Chercheur Qualifié, FNRS, Belgium.

10.1021/jp0012956 CCC: $19.00 
Published on Web 09/07/2000

dots, the spectrum at different locations can be one of several (two or more) distinct types.

The low charging energy cannot be the whole story because the experiments[15,18] clearly show that when the lattice is very compressed, the STM measured density of states becomes symmetric. Therefore, in section 2 we discuss three electronic terms relevant to the description of an array of dots. It is the interplay between these three energies which determines the coupling regime. The problem is more complicated to describe because one has to consider two dimensionless ratios. On the other hand, it makes it richer because with two dimensionless numbers one can have a whole plane of possibilities. In other words, there is a gamut of electronic isomers that are possible[28] and we will comment on this phase diagram.

## 2. Electronic Structure of Arrays of Quantum Dots

Arrays of quantum dots[1,5,10,17] have three features that allow for the control and tuning of the electronic properties of the array. One degree of control is the (relative) experimental ease with which the array can be compressed.[8,9,11] In this way, the extent of overlap of the wave functions of adjacent dots—and hence their electronic coupling—can be varied. Outside of the dot the wave function falls exponentially with distance and so even moderate variations in the spacings of the dots result in large changes in the inter dot coupling.[26] In this paper we will vary the distance between the dots (the lattice spacing) so as to examine different coupling regimes. We will use the coupling as a function of distance as determined by us[25] by fitting to the measured[9] second harmonic response of an array of Ag nanodots.

The second feature is the charging energy of the dot. As already mentioned, it is atypically low. Simple electrostatic considerations suggest that the charging energy will decrease with increasing size of the dot, as is further discussed below. Therefore, the charging energy can be varied via the synthetic procedure that is used to prepare the dots. Values as low as 0.05 eV have been measured for larger metallic dots. In the computations below we shall use the value (0.338 eV) that was measured for the Ag nanodots used in the experiment,[18] which are about 3 nm in size.

Considerable control of the electronic properties is also available through another experimental condition. The synthetic procedure that is used to prepare the dots can be used to govern the spread in sizes of the dots. The distribution cannot be extremely sharp but it can be narrow (about 10%) or broader. Individual dots have discrete electronic states because of their small size, to within which the electron is largely confined. The HOMO is therefore similar to the orbital of a particle in a spherical box of radius $R$. If the potential outside is infinite, the energy can be readily computed analytically and scales as $R^{-2}$. The radius of the dot determines therefore the energy of the highest occupied orbital and also the charging energy. Fluctuations in the size of the dots imply fluctuations in both the energy of the highest occupied orbital of the dot and in the charging energy. The fractional fluctuations are roughly the same because both decrease with increasing size of the dot. The absolute fluctuations in the orbital energies of the dots are far larger because the typical orbital energy is a few eV's i.e., an order of magnitude larger than the charging energy. An important dimensionless variable is the ratio $\Delta\alpha/I$ of the fluctuation in the orbital energy to the charging energy. For a narrow size distribution $\Delta\alpha/I < 1$. It is the opposite case, $\Delta\alpha/I > 1$, where individual dots in the array can exhibit distinct STM responses. The physical reason is that, when $\Delta\alpha > I$, it can be energetically favorable for a (smaller) dot to transfer an electron to an adjacent larger dot, leading to an ionic lattice. It can even be the case that a particularly large dot will accept two electrons. The differently charged dots differ in their charging energy and so an STM probe leads to site-dependent response.

The coupling of adjacent dots depends both on the radius of the dots and on their spacing. The size distribution of the dots can therefore affect this coupling in two different ways: first, directly through the size dependence and, second, indirectly, because a wider size distribution can lead to packing imperfections of the lattice. These variations in the spacings are seen in the STM scan of the lattice.[15]

The actual computation of the orbitals of the lattice has been described in detail in several earlier papers.[27,28] We use a Pariser−Parr−Pople Hamiltonian,[21,30] which includes both the Coulomb blocking (the so-called, Hubbard term) and also a Coulomb repulsion between electrons on adjacent dots

$$H = \sum_{i=1}^{n} \alpha_i \hat{E}_{ii} + \sum_{\substack{i,j \\ \text{near neighbors}}}^{n} \beta_{ij} \hat{E}_{ij} + \frac{1}{2}\sum_{i=1}^{n} I_i \hat{E}_{ii}(\hat{E}_{ii} - 1) + \frac{1}{2}{\sum_{i,j}^{n}}' \gamma_{ij} \hat{E}_{ii} \hat{E}_{jj} \quad (2.1)$$

The Hamiltonian is written in the notation of the unitary group.[12,20] $\hat{E}_{ii}$ is the operator that determines the charge on the site $i$ while $\hat{E}_{ij}$ moves an electron from site $j$ to site $i$. The first two terms in (2.1) are therefore the Hückel (or tight binding) Hamiltonian where $\alpha_i$ is the ionization potential (IP) of the $i$'th dot, $i = 1, ..., n$ and the coupling, $\beta_{ij}$, is the transfer integral, which is nonzero between near neighbors only. $\alpha$, $\beta$, $\gamma$, and $I$ carry labels of the sites because the dots are not equivalent due to the fluctuations in size. As an example, the charging energy can be estimated as $I = e^2/C(R)$, where $C(R)$ is the size dependent finite capacitance of an individual dot, $C(R) = 4\pi\epsilon_0\epsilon R$, where $R$ is the radius of the dot, $\epsilon_0$ is the permittivity of vacuum, and $\epsilon$ is the dielectric constant of the material. It follows that the fluctuation in the charging energy scale as $\delta I = I(\delta R/R)$. The transfer integral $\beta$ depends on the distance $D$ between the dots, and we use the following functional form[25]

$$\beta = (\beta_0/2)(1 + \tanh[(D_0 - D)/4LR]) \quad (2.2)$$

which decays exponentially as $\exp(-D/2RL)$ at large interdot separation. Here there are two sources of variations

$$\delta\beta = \beta(D/2RL)[(\delta D/D) + (\delta R/R)] \quad (2.3)$$

In the computation we draw $R$ and $D$ from a uniform distribution of a specified width about its mean.

Just as the third term in the Hamiltonian (2.1) is the electrostatic repulsion between two electrons on the same site, the last term is the repulsion between two electrons on different sites. The restriction $i \neq j$ is indicated by the prime on the summation sign. The lack of similarity between the third and fourth term is only apparent. It stems from Pauli principle restrictions. Since we use one valence orbital per dot, only valence electrons of opposite spins can occupy the same dot. But there are no such restrictions on the repulsion of electrons on adjacent dots. The magnitude of the electrostatic repulsion is proportional to $I$ but decreases with distance between the dots, so it is less important when the array is highly expanded. On the other hand, in a hexagonal array, each dot has six near neighbors so this term is not negligible. Explicitly, in the distance range $D/2R > 1$, which is of interest here, $\gamma = I/\epsilon(D/$

$2R$). We use a unitary group basis[12,20] to diagonalize the Hamiltonian. In this basis the electrostatic repulsion terms are diagonal. The computational effort is needed only to diagonalize the dot-dot electron-transfer operators $\hat{E}_{ij}$.

It is the explicit inclusion of the electrostatic repulsion energy in the Hamiltonian that will lead to the asymmetry in the density of states. That is, the energetic cost of adding an electron is not the mirror image of the cost of removing an electron. In other words, the Hamiltonian (2.1) does not admit of an orbital picture. The energy of any one electron depends specifically on where the other electrons are and not only on their average field. The computational cost of exactly diagonalizing a Hamiltonian, which contains explicit correlation between different electrons is high. We therefore limit the computations to the smallest hexagonal lattice, which has seven sites. Details about the diagonalization are provided in our earlier papers.[27,28]

The one different technical point in this paper is that, for each lattice of $n$ sites and each interdot separation, we carry out three computations, for $n-1$, $n$, and $n+1$ electrons. In other words, we do not invoke Koopmans theorem.

When the lattice is considerably expanded, the Hamiltonian (2.1) assumes a simpler form because the transfer of electrons from one dot to another can be neglected

$$H \xrightarrow{D/2R > 1} H_{\text{site}} = \sum_{i=1}^{n} \alpha_i \hat{E}_{ii} + \frac{1}{2}\sum_{i=1}^{n} I_i \hat{E}_{ii}(\hat{E}_{ii} - 1) + \frac{1}{2}\sum_{i,j}{}' \gamma_{ij} \hat{E}_{ii} \hat{E}_{jj} \quad (2.4)$$

We refer to this Hamiltonian as $H_{\text{site}}$ because it is diagonal in a site basis set and its eigenvalues can be simply written

$$E_m = \sum_{i=1}^{n} \alpha_i n_i + \frac{1}{2}\sum_{i=1}^{n} I_i n_i(n_i - 1) + \frac{1}{2}\sum_{i,j}{}' \gamma_{ij} n_i n_j \quad (2.5)$$

Here $n_i$ is the number of electrons on site $i$ and for a lattice to which no electron was added or withdrawn $\sum_i n_i = n$. Otherwise, the sum is larger or smaller by unity, depending on the sign of the voltage on the STM tip. Different eigenstates differ in the distribution of charge (and spin) on the different sites. We reiterate that (2.5) and also (2.6) below are not orbital energies but energies of the many electron eigenstates.

A limit that readily provides insight is the very highly expanded lattice. Then the electrostatic repulsion between electrons on different dots can be neglected. The state energies are simply the sum of the energies of the different sites

$$E_m = \sum_{i=1}^{n} \alpha_i n_i + \frac{1}{2}\sum_{i=1}^{n} I_i n_i(n_i - 1)$$

$$= \bar{\alpha}\sum_{i=1}^{n} n_i + \sum_{i=1}^{n} \delta\alpha_i n_i + \frac{1}{2}\sum_{i=1}^{n} I_i n_i(n_i - 1) \quad (2.6)$$

In the second line we wrote the site energy in terms of the mean value $\bar{\alpha}$ and the particular fluctuation at a given site. In other words, $\delta\alpha_i$ is a random number in the range $\pm\delta\alpha$.

Figure 1 shows the energies of the possible (singlet) states of a seven dot hexagonal lattice at very low disorder, $\delta\alpha = I/4$, with six, seven, and eight electrons, respectively. It is emphasized that eq 2.6 and Figure 1 show total (electronic) state energies (and not orbital energies) and that the number of electronic states depends on the number of electrons. We use the convention (sometimes called a highly asymmetric junction)

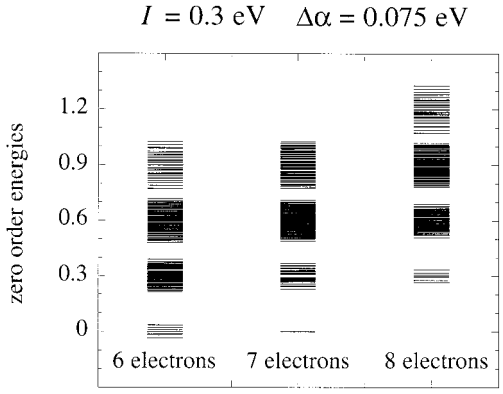


**Figure 1.** Energies of the possible electronic states for a very expanded hexagonal array of seven dots. Equation 2.6 for $\delta\alpha = I/4 = 0.075$ eV. The zero is chosen such that $\bar{\alpha} = 0$. It is emphasized that these are state energies and not orbital energies. The three columns differ in the number of valence electrons, as indicated. There are 490 states for the six and the eight electron cases. For the six electrons, the lowest band, 35 states, is covalent. Each electron is localized on a different dot. The band higher up, 210 states, has one dot with two electrons (and two empty dots). Further up is an even more ionic band, with two dots being negatively charged, etc. The separation between the bands is due to the finite charging energy $I$ and the spread in the energies is due to the fluctuations in the size. When the fluctuations are wider, the bands will begin to overlap, as shown in Figure 2. For the eight electrons, already the lowest band, 35 states, is ionic since one dot has two electrons. The band higher up is doubly ionic, etc.

that the six electron states will be accessed at a negative voltage while the eight electron states are seen at positive voltages. The energy scale in Figure 1 corresponds to a negative voltage for the left column of states and to positive voltage for the right column. The lack of symmetry that we are talking about is that at a given energy we do not have corresponding states.

This failure of Koopmans theorem is easily seen analytically in the limit of a highly expanded lattice, eq 2.6. Consider adding or withdrawing an electron, $\sum_i n_i = n + 1$ or $\sum_i n_i = n - 1$, respectively. The fluctuations in the site energies need to average out, $\sum_i \delta\alpha_i = 0$, but because the sites need not be uniformly occupied, this does not imply $\sum_i n_i \delta\alpha_i = 0$. If there is no charging energy term in (2.6), the change in energy of the state is $\pm\alpha_j$, where $j$ is the site whose occupancy has changed. Say first that the $n$ electrons are evenly distributed over the $n$ sites. With the last term in (2.6), adding an electron to the neutral array means that one site must now be doubly occupied and its energy is higher, by the charging energy $I$. Since we assume that each site is singly occupied, removing an electron does not result in a loss in charging energy. Computational examples, using energies obtained by an exact diagonalization of the full Hamiltonian, are shown in the figures below.

Equations 2.5 or 2.6 imply that the deviations from symmetry (or, in general, deviations from Koopmans theorem) occur primarily for the lower excited states i.e., for low (positive or negative) tip voltages. The reason is that the higher excited states of the uncharged dot are characterized by a nonuniform distribution of charges. Therefore, whether adding or withdrawing an electron one will have charging energy effects. It is only the lowest excited states for which the charges are uniformly distributed, one per site, that it makes a qualitative difference if an extra electron is accommodated or if an existing electron is withdrawn. These lower excited states are but a fraction of the total number of singlet states (35 states out of 490 for six electrons on seven sites, these are the lowest band in the left column of Figure 1) and so the symmetry breaking in never extreme.

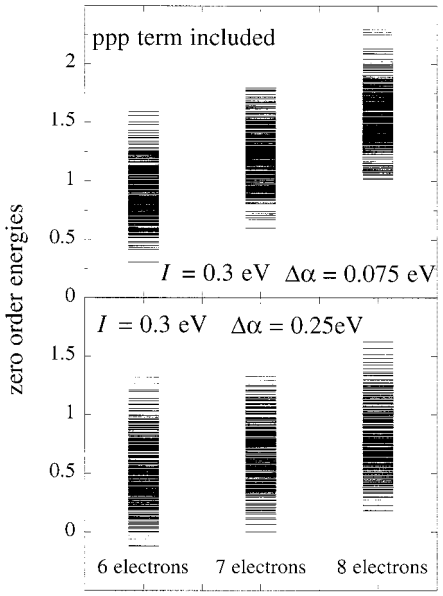


**Figure 2.** Energies of the possible electronic states for a very expanded hexagonal array of seven dots. Same as Figure 1 but the top panel includes electrostatic repulsion between electrons on different dots, see eq 2.5. The bottom panel has higher disorder than in Figure 1. Now the bands discussed in the legend of Figure 1, are overlapping. The extent of disorder shown for the bottom panel is quite realistic.

Figure 1 provides the essence of what we have to say. An STM scan is just a scan of this figure with the technical refinement that each state is weighted by the charge on the site over which the tip is located. See eq 3.1 and also Figure 7, below which is an STM spectrum showing a band structure. Figure 1 is drawn for the simple limit of eq 2.6. Therefore, in Figure 2 we show separately the role of two effects, effects included in the full computation. The top panel is eq 2.5, i.e., including electrostatic repulsion of electrons on different dots. The amount of disorder is the same as in Figure 1, namely low. The bottom panel shows the role of increased disorder, $\delta\alpha \approx I$. Either effect tends to make the energies more uniformly spread. The full computation includes one more term, allowing for electron transfer between adjacent dots.

We caution the reader not to draw the conclusion that we are demolishing Koopmans theorem. We are talking small energy differences, of the order of the charging energy. These are measurable in an STM experiment and hence we need to make corrections for them. But on the whole it is a correction and not a change in perspective. The asymmetry in the density of states that we report below, computed for a realistic Hamiltonian is not much more than 20%. Moreover, it is a correction made necessary by the atypically low value of the charging energy as is special to the case of quantum dots. When the charging energy is far higher, it is not necessary to exactly diagonalize the Hamiltonian (2.1) because states that differ in their energy by the order of $I$ will be only weakly interacting. A second cautionary note concerns the representation of the electronic states of the isolated dots. The computations we show below are for interacting dots, when their coupling, as measured by the magnitude of the transfer integral $\beta$, is finite, cf. eq 2.2. The approximation (2.6) is valid only when $\beta \ll I$. In this limit the dots are isolated, and one knows[2,3,24] that in an STM experiment one can see not only the valence orbital of the dot but also excited states. Hence a physically more correct asymptotic limit is given using an "extended Hückel" representation[13] for the energies of the dots

$$E_m = \sum_{k \text{ extended valence states}} \sum_{i=1}^{n} \alpha_{ik} n_{ik} + \frac{1}{2}\sum_{i=1}^{n} I_i n_i (n_i - 1) \qquad (2.7)$$

Here $k$ sums over all the possible (valence and excited) states of a dot in the energy range of interest and $n_{ik}$ is the occupancy of the $k$th state on the dot $i$. Also in this extended form, the second term ensures an inherent asymmetry in the density of states.

### 3. Scanning Tunneling Spectroscopy

Following the work of Bardeen,[4,7,16] the "density of states" as measured in an STM experiment at the site $i$ is the weighted sum

$$\mathrm{LDOS}_i \equiv \sum_m c_{im} \delta(E_m - E) \qquad (3.1)$$

where $c_{im}$ is the charge on the site $i$ when the system is in the eigenstate $m$ of the Hamiltonian, $c_{im} = \langle m|\hat{E}_{ii}|m\rangle$. $E$ is the energy as determined by the voltage on the tip. In terms of the operator $\hat{E}_{ii}$ that determines the charge on the site, one can formally write the local density of states as

$$\mathrm{LDOS}_i \equiv \mathrm{Tr}[\hat{E}_{ii}\delta(\hat{H} - E)] \qquad (3.2)$$

The eigenenergies in (3.1) that we use are for the $n - 1$ or $n + 1$ electron states of the $n$ site array. (We compute for $n = 7$.) We normalize the LDOS by the number of electrons. The presence of the electrostatic repulsion terms in the Hamiltonian means that these are not in a mirror image relation to one another. This can be seen analytically when the lattice is highly expanded so that eq 2.6 applies. It is also shown in Figure 1.

In the actual computations we approximate the delta function by including all the eigenstates whose energies are within a narrow finite interval $[E - \Delta E/2, E + \Delta E/2]$ with the weight $1/\Delta E$. At a finite temperature $T$ we sum over all states with a Gaussian weight centered about $E$ with a width $kT$ where $k$ is Boltzmann's constant

$$\mathrm{LDOS}_i(T) \equiv \sum_m c_{im} G((E_m - E)/kT) \qquad (3.3)$$

The experiment often takes an average over many sites of the sample. We can mimic this by (i) repeating the computation of the LDOS for a given site but for a different set of size distribution of the dots, while ensuring that the sum of the fluctuations in the site energies averages out, $\sum_i \delta\alpha_i = 0$, and (ii) averaging over all sites.

### 4. Results

Figure 3 is a typical result for the LDOS vs the scanning voltage, for weakly interacting ($D/2R = 1.4$) dots with a narrow size distribution at a low temperature. Shown is the LDOS averaged over the six external sites of a hexagonal array of seven dots, for a narrow (5%) size distribution. The direction of the asymmetry in the LDOS is as in the experiments,[15,18] namely, a higher peak for electron detachment. This is as expected since in the range $D/2R > 1$ one can use the approximate eq 2.5 to argue that for six electrons over seven sites there will be many states without Coulombic repulsion. These states will give rise to a peak at a low energy, as seen in the experiment and in the figure.

The energy scale used in Figure 3 is set for a photoelectron spectrum. Explicitly, we plot the energy of the eigenstate, $E_m$,

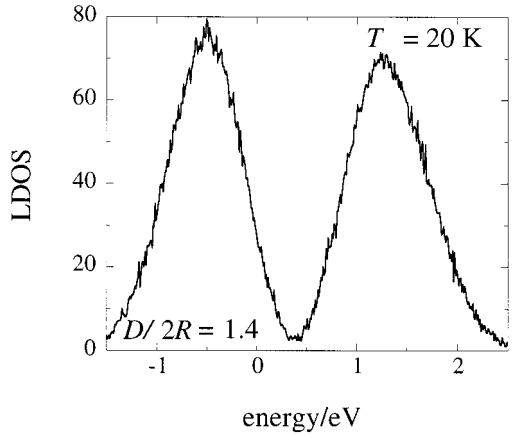


**Figure 3.** Computed charge weighted local density of states, LDOS, eq 3.3, at 20 K for a lattice of seven dots expanded beyond the metal to insulator transition.[29] See text for definition of the energy scale. The results shown are the LDOS averaged over sites 2 to 7, which are the outer sites of the hexagonal array of seven dots. See Figure 4 for site-specific spectra.

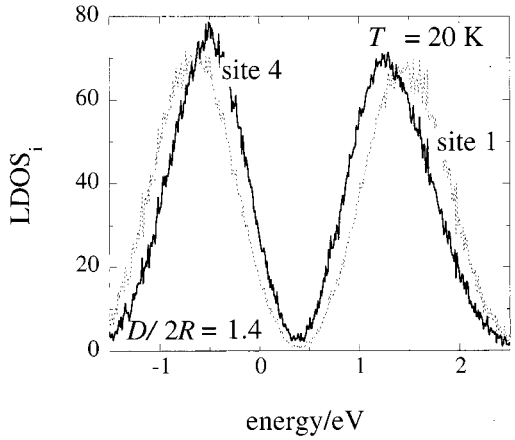


**Figure 4.** Computed charge weighted local density of states, LDOS, eq 3.3, at 20 K as in Figure 3 but for two particular sites. Site 1 is the central site of the hexagonal array of seven dots. This site has strong electrostatic repulsion with six other sites.

minus the ground-state energy of the original seven electron state and set the zero as in Figure 1, i.e., $\bar{\alpha} = 0$. The energies are computed, for each $D/2R$ and a given number of electrons, by a full diagonalization of the Hamiltonian, eq 2.1. The interdot coupling, eq 2.2, is the same as that used in our earlier studies[25,29] of arrays of small Ag nanodots. The fluctuations in size for a given array are kept the same for any number of electrons and for any value of $D/2R$. The computations shown below as Figures 3−7 are an average over 100 samplings of the LDOS. This is to mimic the averaging over many sites in the experimental spectra.

To emphasize the role of the electrostatic repulsion between electrons on adjacent dots, Figure 4 is a computation with the same parameters as Figure 3 but without averaging over the sites. One spectrum shown in Figure 4 is for the central site. This site is not included in the averaging carried out in Figure 3. The spectrum for the central site is not quite similar to Figure 3. This is because the central site has six near neighbors, unlike the external sites which have only three. The spectrum for the central site is thus closer to experimental reality for a hexagonal lattice than Figure 3. One can then ask why do we not compute for a larger hexagonal array, e.g., one of 19 dots where there are two layers of dots surrounding the central one. The answer

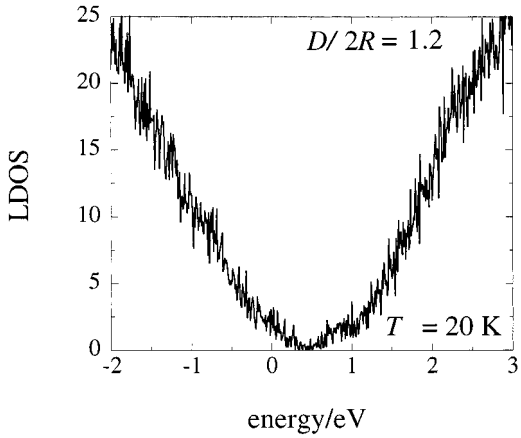


**Figure 5.** Computed charge weighted local density of states, LDOS, eq 3.3, at 20 K for a lattice of seven dots compressed past the metal to insulator transition.[29] The recovery of the mirror image nature of the STM spectrum upon compression is easy to understand. When $D/2R$ decreases, the coupling of the dots increases. By $D/2R \approx 1.3$ the coupling in the Ag nanodots array is comparable to the charging energy (=Mott transition[28]). At closer packings one can begin to neglect the role of the charging energy so that the spectrum of states becomes Hückel-like. Then Koopmans theorem is valid.

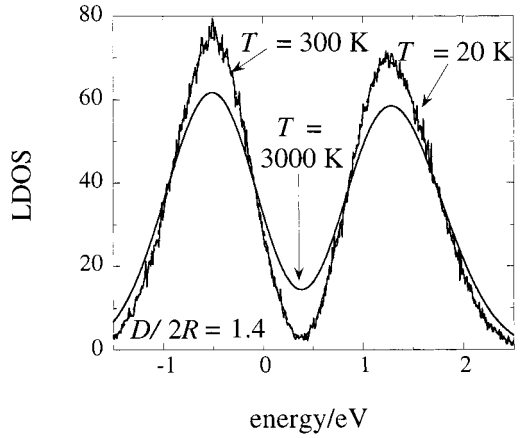


**Figure 6.** Computed charge weighted local density of states, LDOS, eq 3.3, at 20, 300, and 3000 K for a lattice of seven dots expanded beyond the metal to insulator transition.[29] The density of states of a lattice of seven dots is low so, in comparison to experiment, one needs to go to higher temperatures to see a symmetric LDOS. This is because the computed mean spacing of states is higher than it really is so it requires a higher temperature before $kT$ exceeds the mean spacing $\bar{D}$. Therefore, the computations at 20 and 300 K are practically the same whereas in the experiment they will differ. The correct parameter for comparison is $kT/\bar{D}$.

is that, for us, this is computationally intractable. For 19 sites, the Hamiltonian matrix is about 3 billion times 3 billion in size.

The limit of a small $D/2R$ is shown in Figure 5. As in the experiment, once the lattice is compressed and the dots are strongly interacting, the asymmetry disappears. For this close packing the electron-transfer coupling between the dots (as measured by $\beta$) dominates the electrostatic terms and the spectrum becomes metallic like.

Increasing the temperature, Figure 6, allows more states to contribute at a given tip voltage and the asymmetry gradually disappears as the temperature is increased. One can readily estimate the temperature at which the asymmetry will begin to even out. This is when many states contribute in an energy interval of $kT$. Also the gap where there are no states fills up due to thermally assisted transitions.

When the spectrum of excited states of the array is plotted,

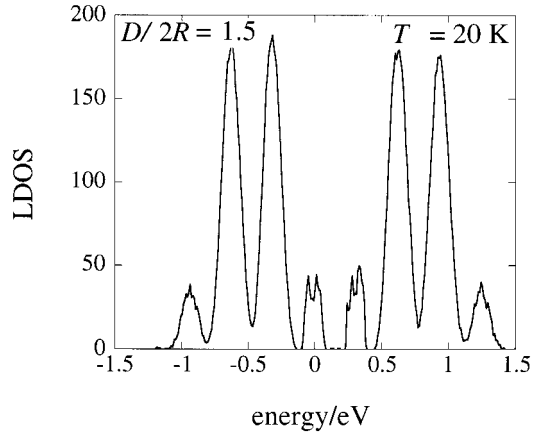


**Figure 7.** Computed charge weighted local density of states, LDOS, eq 3.3, at 20 K for a lattice of seven dots, averaged over all sites. Computed for a narrow size distribution, $\delta\alpha = I/4 = 0.075$ eV, as used also in Figure 1. The bands seen in Figure 1 are clearly resolved in this *computed* STM spectrum.

Figure 1, it is seen that it has several bands. The less compressed is the array, the less overlapping are the bands. A narrow size distribution, such that $\delta\alpha < I$, also serves to keep these bands apart, Figure 1. It is easiest to discuss these bands in the limit $D/2R \gg 1$ where an analytical expression for the energy, (2.5) or (2.6), is available. For six electrons on seven sites, the lowest band of states is the one where there is no more than one electron per site. (There are 35 such (singlet) states for six electrons on seven sites.) These states are not degenerate because the dots are weakly coupled but they are quite close in energy. The next band of states is separated from the lowest band by the charging energy $I$. This is the band where two sites are empty, one site is doubly occupied and four sites are singly occupied. There are 210 such (singlet) states. The coupling between the dots broadens the ground and the first excited band. As the array is compressed and the coupling becomes stronger, there comes a point when the two bands merge. This is analogous to the Mott nonmetal to metal transition. But when the lattice is expanded, the two bands are not overlapping. Higher in energy is the band where two sites are doubly occupied, and even further up, three sites are doubly occupied. In principle, these bands could be resolved by scanning tunneling spectroscopy. Several factors act so as to merge the bands: (i) fluctuations in the site energies (which can be large enough to change the whole picture, so we discuss them further below), (ii) electrostatic repulsion between electrons on different sites, and (iii) coupling between the dots. Figure 7 shows that the band structure can be resolved in the LDOS spectrum.

The role of a broad size distribution deserves a special discussion because qualitatively new features occur. For example, at larger $D/2R$ it is evident from eq 2.6 that the ground state can be ionic. In other words, if because of a fluctuation a site has a low IP, it may be energetically favorable for its electron to be ionized and placed on a site with a high IP. The gain, $\delta\alpha$, in energy can compensate for the additional charging energy. The LDOS is a site-charge weighted density of states, eq 3.1. An ionic ground state could be seen by scanning tunneling spectroscopy as different spectra of different sites. On the other hand, as the energy is scanned, all states and not only the ground state contribute to the LDOS. As we mentioned several times, many excited states are ionic and this is one characteristic of arrays of nanodots. To observe an ionic ground state one needs therefore to look at the low voltage spectrum. Adding an electron will occur at a lower voltage for a site that

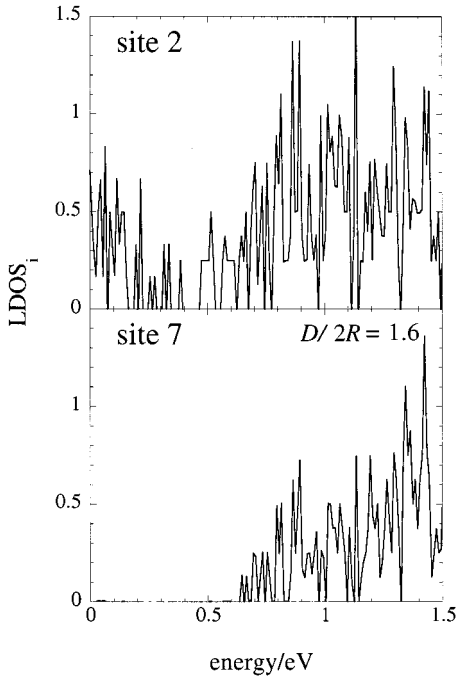


**Figure 8.** Computed charge-weighted local density of states, LDOS, eq 3.3, at 20 K for a lattice of seven dots, same as Figure 3 but without averaging over the sites and with a higher disorder, ($\delta R/R = 0.075$ or $\delta\alpha = 0.75$ eV).

is empty than for one that is singly occupied than for one that is doubly occupied.

That there is, in principle, an effect of a broad size distribution is shown in Figure 8. Plotted in Figure 8 is the LDOS for different sites of a disordered expanded array, without any repeated samplings of the site energies, couplings, etc. The spectrum is therefore bumpy and not continuous looking. The reason for the differences in the spectra of different sites is, as discussed above, due to different occupancies of different sites, for the ground and the lower excited states. Consider, as an example, a site, which because of its larger radius, has a high IP. Such a site will be preferentially occupied not only in the ground state but also in low-lying excited states. It is only for states at far higher energies that such a site will be preferentially empty. In Figure 8, site 2 is of this type. It is doubly occupied and is quite resilient both to acquiring an extra electron or to losing one of its electron. Site 7 is exactly the opposite.

## 5. Electronic Isomers

The computations clearly show that there can be nearly isoenergetic electronic states with a qualitatively different distribution of charges on the sites. It is customary to talk of fluxional molecules with many geometric minima. Here it is the electrons that are fluxional. At a given configuration of the lattice, the electrons can assume different arrangements with comparable energies. The one simple limit is a lattice that is compressed enough that the dot-dot coupling $\beta$ can overcome both the electrostatic and the size disorder effects, $\beta > I$ or $\delta\alpha$. Then the lattice is metallic, meaning that the electrons can be assigned to delocalized molecular orbitals. The electron-transfer coupling is strong enough to overcome both the electrostatic costs of moving the charge and any gap in the IP's of adjacent sites. There are two opposite limits, $\beta < \delta\alpha < I$, for a narrower size distribution and/or higher charging energy and $\beta < I < \delta\alpha$ for a broad size distribution and/or lower charging energy. As can be seen from eq 2.5, in either case there is much scope

for electronic fluxionality but when $I < \delta\alpha$ the scope is richer: For a broad size distribution, very low energy ionic states are possible. The intermediate regime, $\delta\alpha < \beta < I$, is a typical Mott insulator.[19] The dot-dot coupling cannot overcome the charging energy. But another limit,[25,28] $I < \beta < \delta\alpha$, is not as familiar. Here the coupling can overcome the charging effects, but the orbitals are not yet delocalized. One has small domains over which the electrons can move, but overall, they are still localized.

## 6. Concluding Remarks

Scanning tunneling experiments (STM) showing that the density of states of an array of Ag nanodots at low temperatures is asymmetric with respect to adding or removing an electron were recently reported.[15,18] There is no observed asymmetry when the array is more closely packed and/or when the temperature is raised. We have argued[26] that broken symmetry is characteristic of arrays of quantum dots and can be directly observed in the failure of selection rules of optical spectroscopy. STM is a different type of experiment, where electrons are detached or attached. It is analogous to photoelectron spectroscopy and most closely resembles the Ne(gative)−Ne(utral)−Po(sitive) scheme of Wöste and Berry.[6,32] We presented computations of the density of states of an array of Ag nanodots that are in accord with all available experimental observations.

The asymmetry of the tunneling current vs voltage spectrum reflects the asymmetry in the energies of the states of the system. The physical basis of this is the low charging energy of the dots, which is comparable in magnitude to the coupling between adjacent dots. Under such circumstances the electrons are strongly correlated. When the lattice is compressed, the coupling between adjacent dots dominates and one can assign electrons to molecular orbitals. The orbital energy determines the ionization potential or the electron affinity (Koopmans theorem). If the coupling also dominates the fluctuation in the energies of the sites, the molecular orbitals are delocalized and the spectrum is symmetric as for a metal.

At a finite temperature, when more states can contribute to the (charge weighted, local) density of states at a given voltage, the asymmetry is reduced and eventually disappears at a high enough temperature.

**Acknowledgment.** We thank J. R. Heath, S.-H. Kim, and R. S. Williams for many discussions and for detailed information about their experiments and U. Banin and O. Millo for a discussion of STM. This work was supported by the von Humboldt Foundation and used computational facilities provided by SFB 377. F.R. thanks the "Action de Recherche Concertée", Liège University, Belgium.

## References and Notes

(1) Alivisatos, A. P. *Science* **1996**, *271*, 933.

(2) Alperson, B.; Rubinstein, I.; Hodes, G.; Porath, D.; Millo, O. *Appl. Phys. Lett.* **1999**, *75*, 1751.

(3) Banin, U.; Cao, Y.; Katz, D.; Millo, O. *Nature* **1999**, *400*, 542.

(4) Bardeen, J. *Phys. Rev. Lett.* **1961**, *6*, 57.

(5) Bawendi, M. G.; Steigerwald, M. L.; Brus, L. E. *Annu. Rev. Phys. Chem.* **1990**, *41*, 477.

(6) Berry, R. S.; Bonacic-Koutecky, V.; Gaus, J.; Leisner, T.; Manz, J.; Reischl-Lenz, B.; Ruppe, H.; Rutz, S.; Schreiber, E.; Vajda, S.; de Vivie-Riedle, R.; Wolf, S.; Wöste, L. *Adv. Chem. Phys.* **1997**, *101*, 101.

(7) Chen, C. J. Unified Perturbation Theory for STM and SFM. In *Scanning Tunneling Spectroscopy III*; Wiesendanger, R., Güntherodt, H.-J., Eds.; Springer-Verlag: Berlin, 1993; Vol. 29, p 141.

(8) Chen, S.; Ingram, R. S.; Hostetler, M. J.; Pietron, J. J.; Murray, R. W.; Schaaff, T. G.; Khoury, J. T.; Alvarez, M. M.; Whetten, R. L. *Science* **1998**, *280*, 2098.

(9) Collier, C. P.; Saykally, R. J.; Shiang, J. J.; Henrichs, S. E.; Heath, J. R. *Science* **1997**, *277*, 1978.

(10) Collier, C. P.; Vossmeyer, T.; Heath, J. R. *Annu. Rev. Phys. Chem.* **1998**, *49*, 371.

(11) Heath, J. R.; Knobler, C. M.; Leff, D. V. *J. Phys. Chem. B* **1997**, *101*, 189.

(12) *The Unitary Group for the Evaluation of Electronic Energy Matrix Elements*; Hinze, J., Ed.; Springer: Berlin, 1981; Vol. 22.

(13) Hoffmann, R. *Solids and Surfaces*; VCH: New York, 1988.

(14) Hubbard, J. *Proc. R. Soc.* **1963**, *276*, 238.

(15) Kim, S.-H.; Meideiros-Ribeiro, G.; Ohlberg, D. A. A.; Williams, R. S.; Heath, J. R. *J. Phys. Chem. B* **1999**, *103*, 10341.

(16) Lang, N. D. STM Imaging of Single-Atom Adsorbates on Metal. In *Scanning Tunneling Spectroscopy III*; Wiesendanger, R., Güntherodt, H.-J., Eds.; Springer-Verlag: Berlin, 1993; Vol. 29, p 7.

(17) Markovich, G.; Collier, C. P.; Henrichs, S. E.; Remacle, F.; Levine, R. D.; Heath, J. R. *Acc. Chem. Res.* **1999**, *32*, 415.

(18) Medeiros-Ribeiro, C.; Ohlberg, D. A. A.; Williams, R. S.; Heath, J. R. *Phys. Rev. B* **1999**, *59*, 1633.

(19) Mott, N. F. *Metal−Insulator Transitions*; Taylor & Francis: London, 1990.

(20) Paldus, J. Unitary Group Approach to Many-Electron Correlation Problem. In *The Unitary Group for the Evaluation of Electronic Energy Matrix Elements*; Hinze, J., Ed.; Springer: Berlin, 1981; Vol. 22, p 1.

(21) Parr, R. G. *Quantum Theory of Molecular Electronic Structure*; Benjamin: New York, 1963.

(22) Pilar, F. L. *Elementary Quantum Chemistry*; McGraw-Hill: New York, 1968.

(23) *Free Electron Theory of Conjugated Molecules*; Platt, J. R., Ed.; Wiley: New York, 1964.

(24) Porath, D.; Levi, Y.; Tarabiah, M.; Millo, O. *Phys. Rev. B* **1997**, *56*, 9829.

(25) Remacle, F.; Collier, C. P.; Heath, J. R.; Levine, R. D. *Chem. Phys. Lett.* **1998**, *291*, 453.

(26) Remacle, F.; Collier, C. P.; Markovich, G.; Heath, J. R.; Banin, U.; Levine, R. D. *J. Phys. Chem. B* **1998**, *102*, 7727.

(27) Remacle, F.; Levine, R. D. *J. Chem. Phys.* **1999**, *110*, 5089.

(28) Remacle, F.; Levine, R. D. *P. Natl. Acad. Sci. U.S.A.* **2000**, *97*, 553.

(29) Remacle, F.; Levine, R. D. *J. Am. Chem. Soc.* **2000**, *122*, 4084.

(30) Schatz, G. C.; Ratner, M. A. *Quantum Mechanics in Chemistry*; Prentice Hall: New York, 1993.

(31) Stafford, C. A.; DasSarma, S. *Phys. Rev. Lett.* **1994**, *72*, 3590.

(32) Wolf, S.; Sommerer, G.; Rutz, S.; Schreiber, E.; Leisner, T.; Wöste, L.; Berry, R. S. *Phys. Rev. Lett.* **1995**, *74*, 4177.